Low–energy ηd resonance

N. V. Shevchenko[1,3], V. B. Belyaev[1,2], S. A. Rakityansky[2], S. A. Sofianos[2], W. Sandhas[4]
[1] *Joint Institute for Nuclear Research,Dubna, 141980, Russia*
[2] *Physics Dept., University of South Africa, P.O. Box 392, Pretoria 0003, South Africa*
[3] *Physics Dept., Irkutsk State University, Irkutsk 664003, Russia*
[4] *Physikalisches Institut, Universität Bonn, D-53115 Bonn, Germany*

arXiv:nucl-th/9908035v1 10 Aug 1999

Abstract

Elastic ηd scattering is considered within the Alt–Grassberger–Sandhas (AGS) formalism for various ηN input data. A three–body resonant state is found close to the ηd threshold. This resonance is sustained for different choices of the two–body ηN scattering length $a_{\eta N}$. The position of the resonance moves towards the ηd threshold when $\mathrm{Re}\, a_{\eta N}$ is increased, and turns into a quasi-bound state at $\mathrm{Re}\, a_{\eta N} = 0.733\,\mathrm{fm}$.

PACS numbers: 25.80.-e, 21.45.+v, 25.10.+s

One of the main questions of η–meson physics concerns the existence of η–nuclei, a possibility predicted in a pioneering work by Haider and Liu [1]. In this context it is worth mentioning that according to [2] the mean free path of η mesons in a nuclear medium is about 2 fm, *i.e.*, less than the size of a typical nucleus. A necessary condition for the existence of η–nuclei, hence, appears to be satisfied. A further indication is the observation of pionic nuclei (deeply bound pion states inside nuclei) [3], which were predicted theoretically in [4].

Recently, in a number of theoretical investigations based on quite different approaches, such as the mean field approximation [5], the optical model [6], and few–body calculations [7,8], the idea of η–nuclei was given a rather firm ground. Experimentally, after the discouraging attempt of Ref. [9], certain evidence for the existence of η–nuclei was noticed by two groups [10,11]. An additional indication is given by the enhancement of near–threshold η production in the reaction $np \to d\eta$ as reported by the Uppsala group [12]. This observation is most likely to be understood as the effect of a near–threshold bound or resonant ηd state. Moreover, it was suggested [13] that even quite exotic systems containing an η meson and a hyperon (η–hypernuclei) may exist.

Being of interest by itself, the existence of η–nuclei would also shed new light on various fundamental problems of particle physics. For example, the study of η–nuclei would give a clue for understanding the possible restoration of chiral symmetry in a nuclear medium, or its partial restoration which may occur at normal densities $\sim 0.17\,\mathrm{fm}^{-3}$ [14–16]. A further aspect, which makes such systems interesting for other fields of nuclear physics, is the modification of the two–body ηN force by the nuclear medium. Being enhanced due to the resonant character of the ηN interaction, general properties of such modifications should become particularly evident in this case. Especially, the structure of the S_{11} resonance embedded in a nuclear medium may be studied. This would exhibit certain details of the effective Lagrangian models of such a resonance [17], and shed some light, for example, on

chiral models which suggest a reduction of its partial width for decaying into the ηN channel [16], or assume S_{11} to be a quasi-bound state of the K meson and a Σ hyperon [18]. The interesting suggestion of considering S_{11} as a joint manifestation of threshold (casp) and resonance phenomena [19] could also be checked.

In a sense, the problem of choosing the most adequate model for describing the S_{11} resonance is similar to the usual difficulty of choosing the "correct" two–body potential. A reliable judgment on such a choice can be given when this potential (or the resonance) is used in a few–body system where its off-shell properties are exposed. This requires a treatment based on rigorous few–body theory. The Alt–Grassberger–Sandhas (AGS) equations [20], which are employed in this work to calculate the η–deuteron elastic scattering amplitude, belong to this category.

The Faddeev–type coupling of these equations guarantees uniqueness of their solutions. Moreover, as equations for the elastic and rearrangement operators $U_{\alpha\alpha}$ and $U_{\beta\alpha}$, respectively, they are well–defined in momentum space, providing thus the desired scattering amplitudes in a most direct and technically reliable manner. The advantage of working with coupled equations is not only suggested by questions of uniqueness, but also by the relevance of rescattering effects. Indeed, in recent calculations of η–photoproduction from the deuteron it was found that rescattering terms give a significant contribution to the corresponding amplitude [21].

Let the η meson be denoted as particle 1 and the two nucleons as particles 2 and 3. With the momentum $\mathbf{q}_1$ of the meson relative to the center of mass of the nucleons in the deuteron state $|\psi_d\rangle$, the free ηd channel state is given by

$$|\psi_d; \mathbf{q}_1\rangle = |\psi_d\rangle|\mathbf{q}_1\rangle \ , \tag{1}$$

its normalization being chosen as

$$\langle\psi_d; \mathbf{q}_1'|\psi_d; \mathbf{q}_1\rangle = \delta(\mathbf{q}_1' - \mathbf{q}_1) \ . \tag{2}$$

In terms of the AGS transition operator U_{11} the ηd elastic scattering amplitude is represented as

$$f(\mathbf{q}_1', \mathbf{q}_1) = -(2\pi)^2 M_1 \langle\psi_d; \mathbf{q}_1'|U_{11}(z)|\psi_d; \mathbf{q}_1\rangle \ , \tag{3}$$

with the on–energy–shell conditions $|\mathbf{q}_1'| = |\mathbf{q}_1|$ and $z = E_d + q_1^2/2M_1 + i0$. Here M_1 is the reduced mass of particle 1 and the (23) subsystem, $1/M_1 = 1/m_1 + 1/(m_2 + m_3)$.

The elastic transition operator U_{11} satisfies the set of AGS equations

$$U_{\beta\alpha}(z) = (1 - \delta_{\beta\alpha})G_0^{-1}(z) + \sum_{\gamma=1}^{3}(1 - \delta_{\beta\gamma})T_\gamma(z)G_0(z)U_{\gamma\alpha}(z) \ , \tag{4}$$

with $G_0(z)$ being the free resolvent (Green's operator) of the three particles involved. This set of equations couples all 3×3 elastic and rearrangement operators $U_{\alpha\alpha}$ and $U_{\beta\alpha}$. Here each of the subscripts runs through the values 1,2 and 3, indicating the two–fragment partitions (1,23), (2,31) and (3,12) respectively. Therefore, U_{11} describes the elastic transition 1(23)→1(23), while U_{21} represents the rearrangement process 1(23)→2(13).

In accordance with Eq.(1), we denote by $\mathbf{q}_\alpha$ the momentum of particle α relative to the center of mass of the $(\beta\gamma)$ subsystem, and by M_α the corresponding reduced mass. The internal momentum of this subsystem is denoted as $\mathbf{p}_\alpha$. Conventionally, this complementary notation is also used to label the two–body T–operator $t_\alpha(z)$ of the $(\beta\gamma)$ pair, for instance $t_1(z) = t_{NN}(z)$. It should be noticed, however, that it is not this genuine two–body operator which enters the AGS equations, but the operator

$$T_\alpha(z) = t_\alpha(z - \hat{\mathbf{q}}_\alpha^2/2M_\alpha) \ , \tag{5}$$

which is to be understood as the two–body operator embedded in the three–body space, with the relative kinetic energy operator $\hat{\mathbf{q}}_\alpha^2/2M_\alpha$ of particle α being subtracted from the total energy variable z. Considered in momentum space, Eq.(5) thus reads

$$\langle \mathbf{p}'_\alpha, \mathbf{q}'_\alpha | T_\alpha(z) | \mathbf{p}_\alpha, \mathbf{q}_\alpha \rangle = \delta(\mathbf{q}'_\alpha - \mathbf{q}_\alpha) \langle \mathbf{p}'_\alpha | t_\alpha(z - q_\alpha^2/2M_\alpha) | \mathbf{p}_\alpha \rangle \ . \tag{6}$$

Since we are interested in ηd collision the subscript α is fixed to 1. Instead of the 9 equations of system (4) we therefore have to consider only the three equations

$$\begin{aligned} U_{11}(z) = & \quad T_2(z)G_0(z)U_{21}(z) + T_3(z)G_0(z)U_{31}(z) \ , \\ U_{21}(z) = & \ G_0^{-1}(z) + T_1(z)G_0(z)U_{11}(z) + T_3(z)G_0(z)U_{31}(z) \ , \\ U_{31}(z) = & \ G_0^{-1}(z) + T_1(z)G_0(z)U_{11}(z) + T_2(z)G_0(z)U_{21}(z) \ , \end{aligned} \tag{7}$$

involving the operator U_{11} which determines the elastic amplitude (3). In momentum space the system (7) consists, after partial wave decomposition, of three coupled two–dimensional integral equations. It is customary to reduce the dimension of these equations by approximating or representing the two–body T–operators in separable form,

$$t_\alpha(z) = |\chi_\alpha\rangle \tau_\alpha(z) \langle \chi_\alpha| \ , \qquad \alpha = 1, 2, 3 \ , \tag{8}$$

or, according to (5), by

$$T_\alpha(z) = |\chi_\alpha\rangle \tau_\alpha(z - \hat{\mathbf{q}}_\alpha^2/2M_\alpha) \langle \chi_\alpha| \ , \qquad \alpha = 1, 2, 3 \ . \tag{9}$$

Inserting this representation in the AGS equations (4) and sandwiching them between $\langle \chi_\beta|$ and $|\chi_\alpha\rangle$ they take the form

$$X_{\beta\alpha}(z) = (1 - \delta_{\beta\alpha}) \langle \chi_\beta | G_0(z) | \chi_\alpha \rangle + \sum_{\gamma=1}^{3} (1 - \delta_{\beta\gamma}) \langle \chi_\beta | G_0(z) | \chi_\gamma \rangle \tau_\gamma(z - \frac{\hat{\mathbf{q}}_\gamma^2}{2M_\gamma}) X_{\gamma\alpha}(z) \ . \tag{10}$$

The three–body operators $U_{\beta\alpha}$, hence, are replaced by the effective two–body operators

$$X_{\beta\alpha}(z) = \langle \chi_\beta | G_0(z) U_{\beta\alpha}(z) G_0(z) | \chi_\alpha \rangle \tag{11}$$

which act exclusively on the relative momentum states $|\mathbf{q}_\alpha\rangle$. After partial wave decomposition we then end up with one-dimensional integral equations.

The form-factor $|\chi_1\rangle$ in the NN operator t_1 is related to the deuteron wave function $|\psi_d\rangle$ according to

$$|\psi_d;\mathbf{q}_1\rangle = G_0\left(q_1^2/2M_1 + E_d\right)|\chi_1\rangle|\mathbf{q}_1\rangle \ , \tag{12}$$

where E_d is the deuteron energy. The on-energy-shell matrix element in (3), thus, can be written in the form

$$f(\mathbf{q}_1',\mathbf{q}_1) = -(2\pi)^2 M_1 \langle \mathbf{q}_1'|X_{11}(z)|\mathbf{q}_1\rangle \ . \tag{13}$$

In other words, the set of equations (10) provides the elastic amplitude we are interested in.

In the present case there are further simplifications caused by the identity of the nucleons. Indeed, the momentum representation of X_{31}, τ_3, $|\chi_3\rangle$ and of X_{21}, τ_2, $|\chi_2\rangle$ respectively are of the same functional form. This reduces the three equations involving X_{11} to the following pair

$$\begin{aligned} X_{11}(z) &= 2\langle\chi_1|G_0(z)|\chi_2\rangle\tau_2\left(z-\hat{\mathbf{q}}_2^2/2M_2\right)X_{21}(z) \ , \\ X_{21}(z) &= \langle\chi_2|G_0(z)|\chi_1\rangle + \langle\chi_2|G_0(z)|\chi_1\rangle\tau_1\left(z-\hat{\mathbf{q}}_1^2/2M_1\right)X_{11}(z) \\ &\quad +\langle\chi_2|G_0(z)|\chi_2\rangle\tau_2\left(z-\hat{\mathbf{q}}_2^2/2M_2\right)X_{21}(z) \ . \end{aligned} \tag{14}$$

The S–wave nucleon–nucleon separable potential is adopted from Ref. [22] with its parameters slightly modified to be consistent with more recent NN data (see Ref. [8]). The η–nucleon T–matrix is taken in the form

$$t_{\eta N}(p',p;z) = (p'^2+\alpha^2)^{-1}\frac{\lambda}{(z-E_0+i\Gamma/2)}(p^2+\alpha^2)^{-1} \tag{15}$$

consisting of two vertex functions and the S_{11}-propagator in between [7]. It corresponds to the process $\eta N \to S_{11} \to \eta N$ which at low energies is dominant. The range parameter $\alpha = 3.316$ fm^{-1} was determined in Ref. [23], while E_0 and Γ are the parameters of the S_{11} resonance [24],

$$E_0 = 1535\,\mathrm{MeV} - (m_N + m_\eta) \ , \qquad \Gamma = 150\,\mathrm{MeV} \ .$$

The strength parameter λ is chosen to reproduce the η–nucleon scattering length $a_{\eta N}$,

$$\lambda = \frac{\alpha^4(E_0 - i\Gamma/2)}{(2\pi)^2\mu_{\eta N}}a_{\eta N} \ . \tag{16}$$

It is customary to use complex $a_{\eta N}$ the imaginary part of which accounts for the flux losses into the πN channel. The value of $a_{\eta N}$ is not accurately known. Different analyses [25] provided for $a_{\eta N}$ values in the range

$$0.27\ \mathrm{fm} \le \mathrm{Re}\, a_{\eta N} \le 0.98\ \mathrm{fm} \ , \qquad 0.19\ \mathrm{fm} \le \mathrm{Im}\, a_{\eta N} \le 0.37\ \mathrm{fm} \ . \tag{17}$$

Recently, however, most of the authors agreed that $\mathrm{Im}\, a_{\eta N}$ is around 0.3 fm. But for $\mathrm{Re}\, a_{\eta N}$ the estimates are still very different (compare, for example, Refs. [26] and [27]). We, therefore, fixed $\mathrm{Im}\, a_{\eta N}$ to 0.3 fm and did calculations for several values of $\mathrm{Re}\, a_{\eta N}$ within the above interval.

We solved Eqs. (14) for ηd collision energies varying from zero (ηd-threshold, $z = E_d$) up to 22 MeV. As is well known (see, for example, [28]), the kernels of Eqs.(14), when expressed

in momentum representation, have logarithmic singularities for $z > 0$. These singularities stem from the Green's functions which in their denominators involve two terms $q_\alpha^2/2M_\alpha$ and $p_\alpha^2/2\mu_\alpha$ corresponding to the pair of Jacobi momenta. The singularities appear after angular integration, and their position depends on the values of p_α and q_α (the so-called moving singularities). In the numerical procedure, we handle it with the method suggested in Ref. [29]. The main idea of this method consists in expanding the unknown solutions (in the area covering the singular points) in certain polynomials and subsequent analytic integration of the singular part of the kernels.

The results of our calculations are presented in Figs. 1–5 and in Table I. In Figs. 1 and 2 the energy dependence of the ηd phase-shifts for five different choices of $\mathrm{Re}\, a_{\eta N}$ is shown, namely, for 0.55 fm, 0.65 fm, 0.725 fm, 0.75 fm, and 0.85 fm. The larger this value, the stronger is the ηN attraction. The change in the character of these curves, hence, reflects the growth of the attractive force between the η meson and the nucleon. The lower three curves for $\mathrm{Re}\, \delta_{\eta d}$ corresponding to the smaller values of $\mathrm{Re}\, a_{\eta N}$ start from zero, the two curves corresponding to the strong attraction start from π. According to Levinson's theorem, the phase shift at threshold energy is equal to the number of bound states n times π. We found that the transition from the lower family of the curves to the upper one happens at $\mathrm{Re}\, a_{\eta N}$=0.733 fm. Therefore, the ηN force, which generates $\mathrm{Re}\, a_{\eta N} > 0.733$ fm, is sufficiently attractive to bind η inside the deuteron. This is the first conclusion of our calculations.

The second conclusion concerns the peaks in the energy dependence of the total elastic cross-section (see Fig. 4), indicating that a resonance appears in the ηd–system. Of course, not every maximum of the cross-section is a resonance, but the Argand plots, shown in Fig. 5, prove that the maxima we found are resonances. Their positions and widths for various choices of $\mathrm{Re}\, a_{\eta N}$ are given in Table I. It should be noted that, while the resonance energy is determined in our calculations exactly (as the maximum of the function $\sin^2 \mathrm{Re}\, \delta_{\eta d}$), the corresponding width is obtained by fitting the cross-section with a Breit–Wigner curve. Therefore, the values of $\Gamma_{\eta d}$ given in Table I should be considered only as rough estimates.

The presence of a resonance before a quasi-bound state appears is not surprising. With increasing attraction the poles of the S-matrix should move in the complex plane from the resonance area to the quasi-bound state area. This is exactly what our calculations indicate. In Ref. [8] we showed that such transition of the pole happens when $\mathrm{Re}\, a_{\eta N}$ changes from 0.25 fm to 1 fm. Here we found more exactly that it happens at $\mathrm{Re}\, a_{\eta N}$=0.733 fm.

The resonant behaviour of ηd elastic scattering should be seen in various processes involving ηd–system in their final states, such as $\gamma d \to d\eta$ and $np \to d\eta$. Recent measurements [12] of the η–production in the np collisions reveal a bump of the cross–section for the reaction $np \to d\eta$ at a c.m. energy below 5 MeV. If we suppose that the energy dependence of this cross–section is mainly determined by the final state interaction, then this bump can be explained by the existence of an ηd resonance. Moreover, since the bump was observed below 5 MeV, the resonance positions given in Table I imply the rough lower bound $\mathrm{Re}\, a_{\eta N} \geq 0.75$ fm. For a reliable estimate, however, one has to perform an explicit calculation of the corresponding cross-section. A recent analysis [27] of this reaction with a non-resonant final state interaction is consistent with the data of Ref. [12] only if $\mathrm{Re}\, a_{\eta N} = 0.30$ fm. Finally, it is interesting to note that there is tentative evidence for a similar bump in the low–energy region in the reaction $\gamma d \to X\eta$ [30].

ACKNOWLEDGMENTS

Financial support from Deutsche Forschungsgemeinschaft, NATO (grant #CR-GLG970110), INTAS (grant #96-0457), International Center for Fundamental Physics (Moscow), Russian Foundation for Basic Research, National Research Foundation of South Africa and the Joint Institute for Nuclear Research (Dubna) is greatly appreciated.

REFERENCES

[1] Q. Haider and L. C. Liu , Phys. Rev. Lett. B **172**, 257 (1986).
[2] M. Röbig-Landau *et al.*, Phys. Lett. B **373**, 45 (1996).
[3] T.Yamazaki et al. Z. Phys., A **355**, 219 (1996).
[4] H. Toki and T. Yamazaki, Phys. Lett. B **213**, 129 (1988).
[5] K. Tsushima, D. H. Lee, A. W. Thomas, K. Saito, e-print LANL, nucl-th/9806043v2 (1998); K. Saito, K. Tsushima, and A. W. Thomas, e-print LANL, nucl-th/9811031 (1998).
[6] J. Kulpa, S. Wycech, A. M. Green, e-print LANL, nucl-th/9807020 (1998).
[7] S. A. Rakityansky, S. A. Sofianos, M. Braun, V. B. Belyaev, and W. Sandhas, Phys. Rev. C **53**, R2043 (1996).
[8] N. V. Shevchenko, S. A. Rakityansky, S. A. Sofianos, V. B. Belyaev, and W. Sandhas, Phys. Rev. C **58**, R3055 (1998).
[9] R. E. Chrien et al. Phys. Rev. Lett. **60**, 2595 (1988).
[10] N. Willis *et al.*, Phys. Lett. B **406**, 14 (1997).
[11] G. A. Sokol *et al.*, e-print LANL, nucl-th/9812007 (1998).
[12] H. Calen et al., Phys. Rev. Lett., **80**, 2069 (1998).
[13] V. V. Abaev and B. M. K. Nefkens, Phys. Rev., C **53**, 358 (1996).
[14] T. Hatsuda and T. Kunihiro, Phys. Rep. **247**, 221 (1994).
[15] G. E. Brown and M. Rho, Phys. Rep. **269**, 333 (1996).
[16] H. Kim, D. Jido and M. Oka, e-print LANL, hep-ph/9806275 (1998).
[17] M. Benmerrouche et al., Phys. Rev., D **51** 3237 (1995).
[18] N. Keiser, T. Waas, W. Weise, Nucl. Phys. A **612**, 297 (1997).
[19] G. Höhler, talk at 7th Int. Symposium at Vancouver (Jul. 28 - Aug. 1, 1997)
[20] E. O. Alt, P. Grassberger, and W. Sandhas, Nucl. Phys. B **2**, 167 (1967).
[21] F. Ritz and H. Arenhövel, Phys. Lett. B **447**, 15 (1999).
[22] H. Garcilazo, Lett.Nuovo Cim., **28**, 73 (1980).
[23] C. Bennhold and H. Tanabe, Nucl. Phys., A **530**, 625 (1991).
[24] Particle Data Group, Phys. Rev. D **50(3)**, 1319 (1994).
[25] M. Batinic, I. Slaus, A. Svarc, Phys. Rev. C **52**, 2188 (1995).
[26] A. M. Green, S. Wycech, Phys. Rev., C **55**, R2167 (1997).
[27] V. Yu. Grishina, L. A. Kondratyuk, M. Buescher, C. Hanhart, J. Haidenbauer, J. Speth, e-print LANL, nucl-th/9905049, (1999).
[28] V. B. Belyaev, *Lectures in Few-Body Systems*, Springer Verlag
[29] F. Sohre and H. Ziegelman, Phys. Lett. B **34**, 579 (1971).
[30] J. Weiss (University of Giessen), *privat communication* (1999).

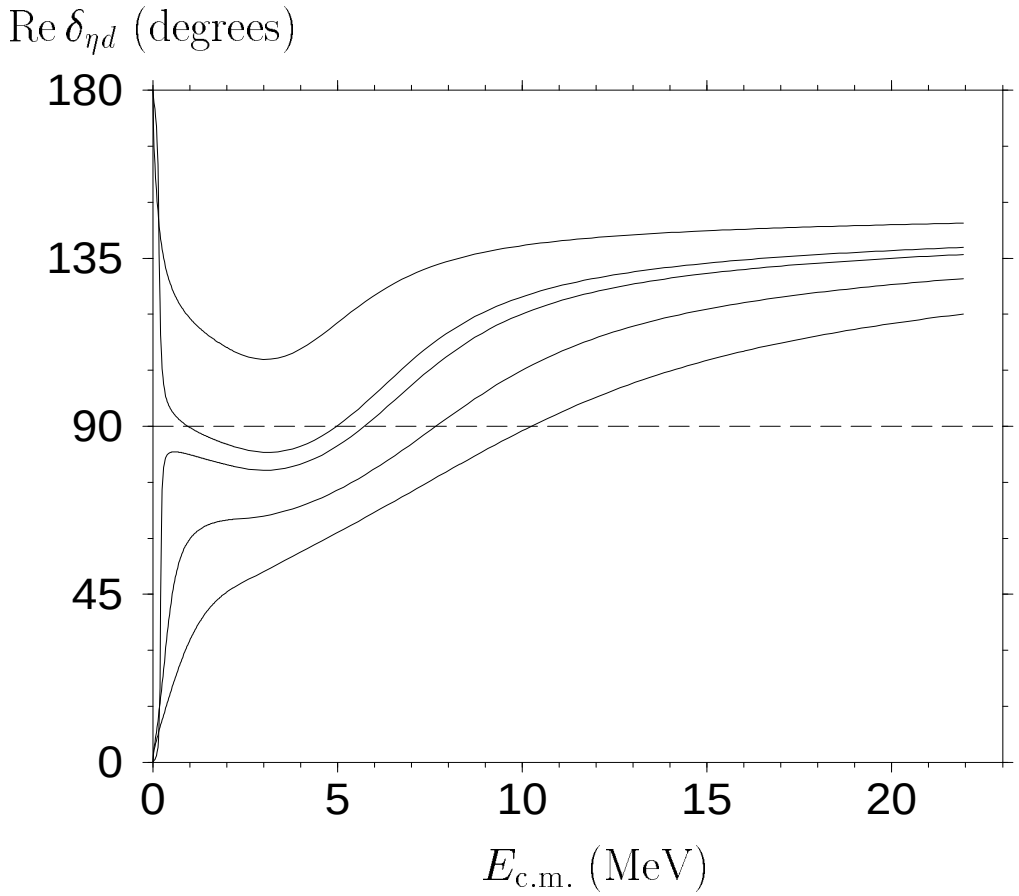


FIG. 1. Real part of the η-deuteron phase-shift as a function of the collision energy. The five curves correspond (starting from the lowest one) to $\mathrm{Re}\, a_{\eta N}$= 0.55 fm, 0.65 fm, 0.725 fm, 0.75 fm, and 0.85 fm.

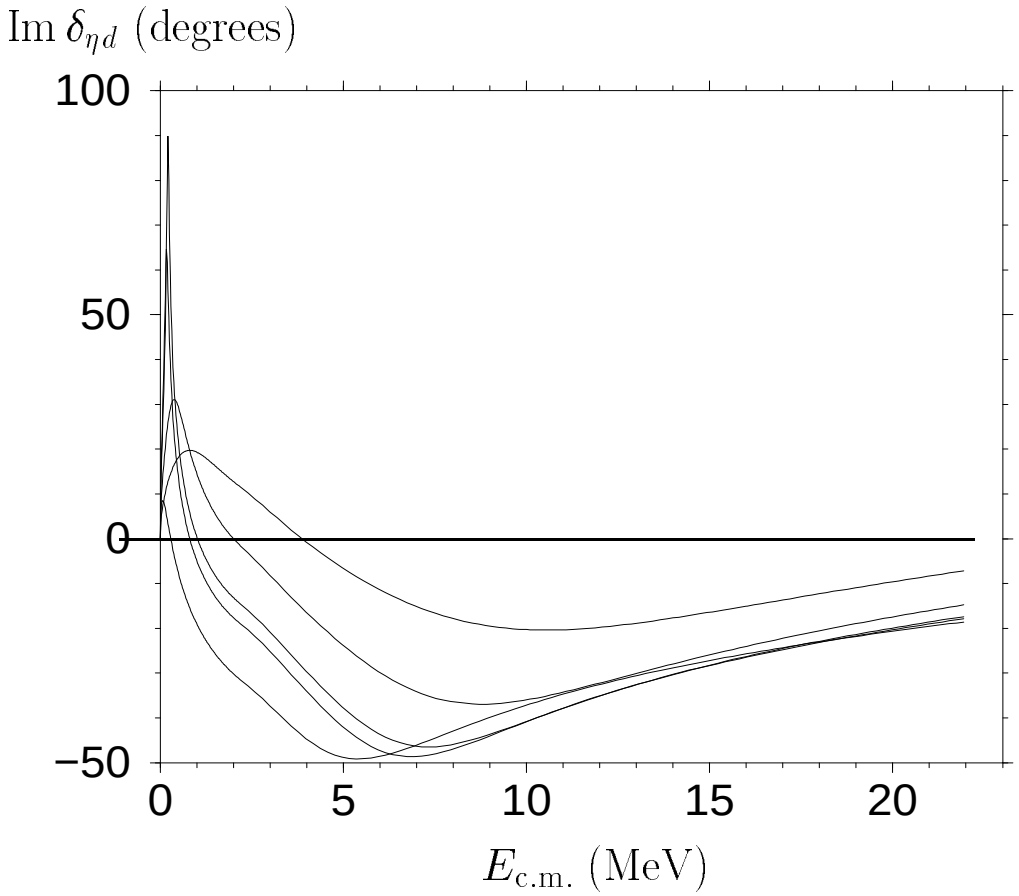


FIG. 2. Imaginary part of the η-deuteron phase-shift as a function of the collision energy. The curves correspond to the same choices of the $\mathrm{Re}\, a_{\eta N}$ as in Fig. 1. Within 1 MeV to 6 MeV, where the curves do not intersect, the lowest one corresponds to $\mathrm{Re}\, a_{\eta N}$=0.85 fm, and every next curve above it corresponds to a smaller $\mathrm{Re}\, a_{\eta N}$.

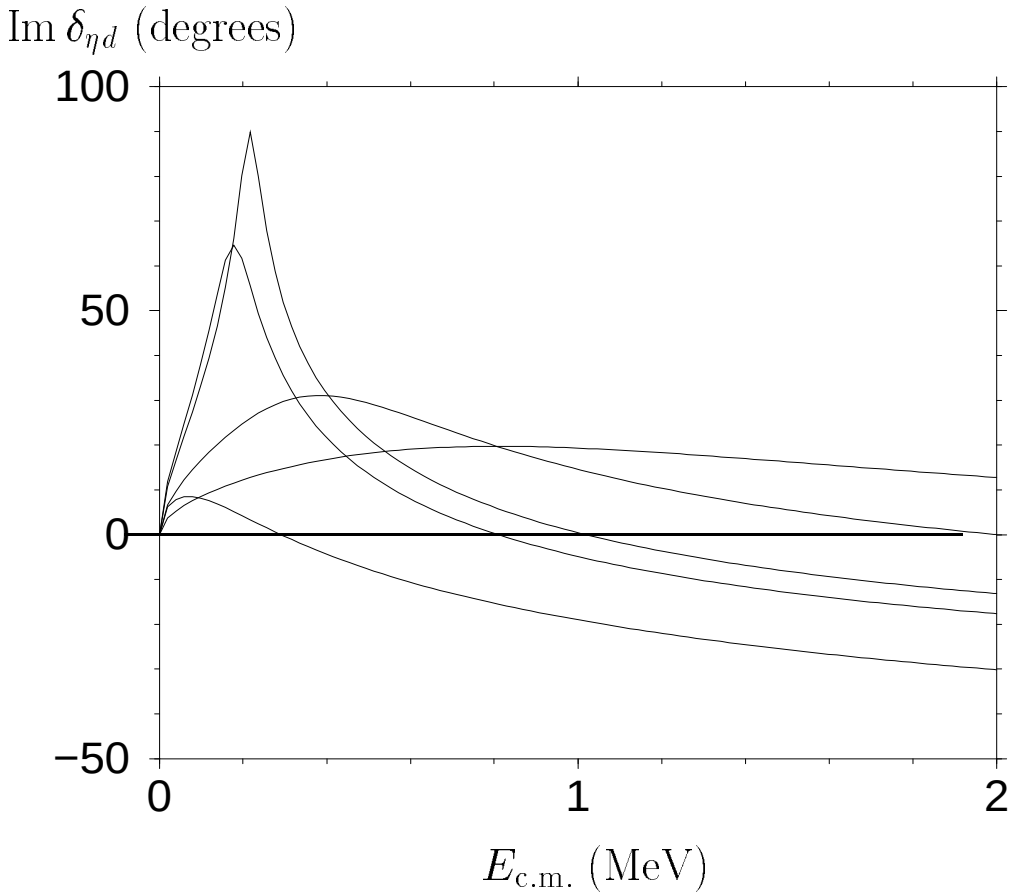


FIG. 3. A magnified fragment of Fig. 2.

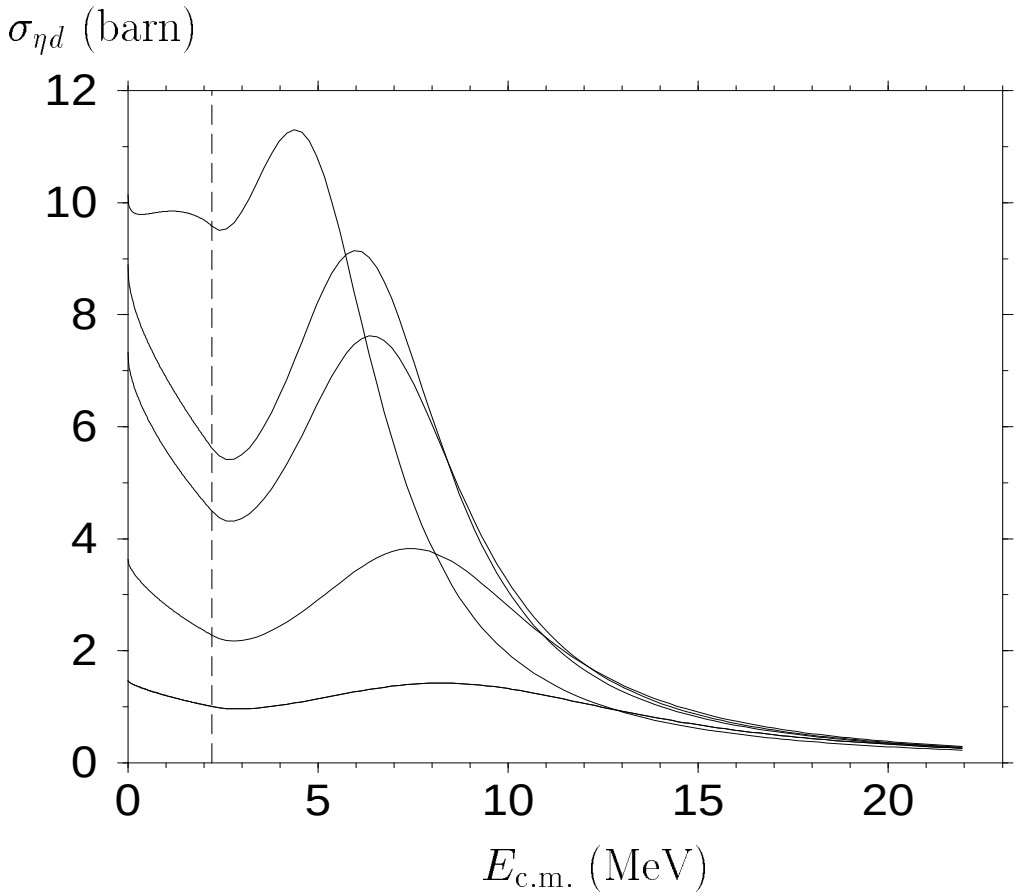


FIG. 4. Total cross–section (integrated over the angles) for elastic η–deuteron scattering as a function of collision energy. The five curves correspond (starting from the lowest one) to $\mathrm{Re}\, a_{\eta N}=$ 0.55 fm, 0.65 fm, 0.725 fm, 0.75 fm, and 0.85 fm. The dashed line indicates the deuteron break-up threshold.

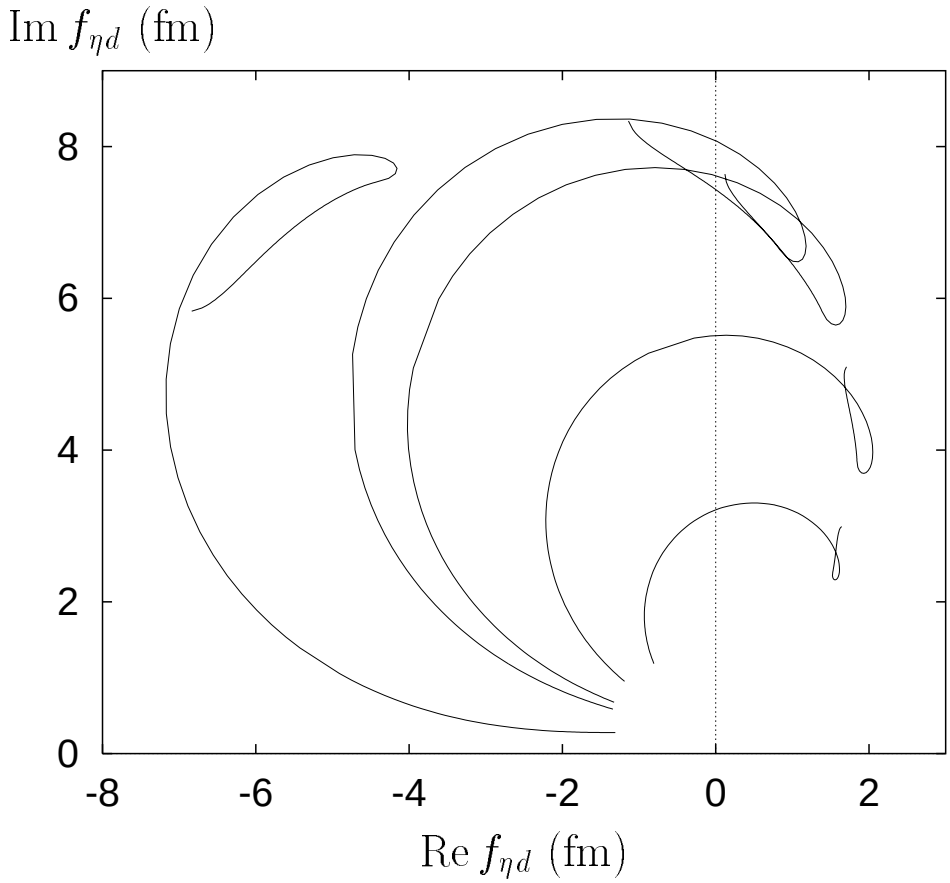


FIG. 5. Argand plot for the ηd elastic scattering amplitude in the energy interval from 0 to 22 MeV. The five curves correspond (from right to left) to $\mathrm{Re}\, a_{\eta N}$= 0.55 fm, 0.65 fm, 0.725 fm, 0.75 fm, and 0.85 fm. When the energy increases the corresponding points move anticlockwise.

TABLES

$\mathrm{Re}\, a_{\eta N}$ (fm)	$E_{\eta d}^{\mathrm{res}}$ (MeV)	$\Gamma_{\eta d}$ (MeV)
0.55	8.24	9.15
0.65	7.46	8.45
0.675	7.14	7.61
0.70	6.79	6.90
0.725	6.41	6.31
0.75	6.01	5.87
0.85	4.39	5.79
0.90	3.73	6.81

TABLE I. Energy and width of the ηd resonance for various choices of $\mathrm{Re}\, a_{\eta N}$.